Remanent magnetization and coercivity of rocks under hydrostatic pressure up to 1.4 GPa

François Demory, Pierre Rochette, Jérôme Gattacceca, Thomas Gabriel, Natalia Bezaeva

Remanent magnetization and coercivity of rocks under hydrostatic pressure up to 1.4 GPa

F. Demory,[1] P. Rochette,[1] J. Gattacceca,[1,2] T. Gabriel,[1] and N. S. Bezaeva[3]

Received 14 May 2013; revised 9 July 2013; accepted 14 July 2013; published 6 August 2013.

[1] We designed an Isothermal Remanent Magnetization (IRM) acquisition system based on permanent magnets and sized to accommodate an amagnetic hydrostatic pressure cell. This pressure cell fits in a superconducting rock magnetometer, allowing for the measurement of remanent magnetization of pressurized samples. With this system, we determined the coercivity of remanence (B_{cr}) at different hydrostatic pressures up to 1.4 GPa for rock and dispersed mineral samples with various magnetic mineralogy and domain state. IRM and B_{cr} are nearly identical before compression and after decompression, indicating no permanent changes in the magnetic properties during pressure cycling. Hydrostatic pressure up to 1.4 GPa does not significantly increases IRM under pressure except for multidomain pyrrhotite and magnetite which show an increase of about 40%. Relative increase of B_{cr} under pressure is mild, except for a near single domain titanomagnetite where B_{cr} doubles.
Citation: Demory, F., P. Rochette, J. Gattacceca, T. Gabriel, and N. S. Bezaeva (2013), Remanent magnetization and coercivity of rocks under hydrostatic pressure up to 1.4 GPa, *Geophys. Res. Lett.*, *40*, 3858–3862, doi:10.1002/grl.50763.

1. Introduction

[2] Investigating the magnetic properties of minerals under high pressures has two main goals. First, during high velocity collision, the instantaneous high pressure produced by the impact can change the magnetic properties of magnetic minerals within the impacted body. Many studies have shown the effects of impact on the target materials magnetization [e.g., *Gattacceca et al*., 2007]. In addition to magnetic mineral deformation, the temporary change of magnetic properties will induce the acquisition of a pressure-induced remanent magnetization in the ambient field and a demagnetization of previous natural remanent magnetization. Consequently, this will influence the characteristics of the magnetic anomaly produced on the planetary surface by the impact. Impact pressures can reach over 100 GPa, but at such high pressure, thermal effects likely erase the pressure effects. On the other hand, impact pressures of less than 5 GPa produce a negligible thermal effect and little deformation [*Melosh*, 1989]. Second, modeling of large scale magnetic anomalies measured by satellite around Earth and Mars implies deeply buried (e.g., up to 50 km [see *Arkani-Hamed and Strangway*, 1987; *Frost and Shive*, 1986; *Voorhies et al*., 2002]) magnetic bodies. Their magnetic properties and natural magnetization probably differ from those measured at atmospheric pressure. The effect of temperature was already considered [e.g., *Dunlop and Arkani-Hamed*, 2005] but little was done for taking hydrostatic pressures into consideration. The range of relevant pressure on Earth is up to 1.5 GPa, i.e., the lithostatic pressure at 50 km depth. A number of studies have been devoted to the effect of uniaxial pressure in a lower pressure range [e.g., *Pozzi*, 1975; *Revol et al*., 1977; *Martin and Noel*, 1988], but the magnetic effect of deviatoric pressure is something rather independent of the hydrostatic pressure effect [*Nagata*, 1966]. Moreover, as soon as deviatoric stress is used, nonelastic irreversible strain may be generated, leading to other mechanisms of magnetization changes [e.g., *Borradaile*, 1997].

[3] Up to now, studies led on the effects of high pressures on magnetic properties have used diamond [*Gilder et al*., 2002] or moissanite anvil cell [*Gilder et al*., 2004; *Gilder and Le Goff* 2008; *Gilder et al*., 2011], up to 6 GPa. Despite characteristics close to hydrostatic conditions, the use of anvil cells with a solid confining media implies deviatoric stresses which necessarily produce magnetic mineral deformation. The existence of nonhydrostatic deviatoric stresses is evidenced in these experiments by the dependence of the results on the maximum compression axis [*Gilder and Le Goff*, 2008] and by direct pressure measurements [*Gilder et al*., 2011]. This deviatoric component has been quantified for diamond anvil cells: it may reach 10% of the pressure at 1 GPa [*Wu and Basset*, 1993]. Although deviatoric stress and strain are also possible in deep crustal conditions, the much lower values of maximum deviatoric stress and strain rate, as well as the healing effect of temperature on strain-induced defects indicate that purely hydrostatic experiments may be a better analog for natural in situ conditions.

[4] The present study presents the production and measurement of isothermal remanent magnetization (IRM) for different samples in a pressure cell with liquid confining media at pressures up to 1.4 GPa, as well as stepwise backfield demagnetization to determine the coercivity of the remanence. Our goal is to characterize the effect of pressure on rock magnetic properties avoiding irreversible magnetic mineral deformation.

2. Material and Experimental Protocol

[5] From the set of samples previously investigated by *Bezaeva et al*. [2010], we selected those containing

Additional supporting information may be found in the online version of this article.

[1]Aix-Marseille Université, CNRS, IRD, CEREGE UM34, 13545 Aix en Provence, France.
[2]Department of Earth, Atmospheric, and Planetary Sciences, Massachusetts Institute of Technology, Cambridge, Massachusetts, USA.
[3]Earth Physics Department, Faculty of Physics, M.V. Lomonosov Moscow State University Leninskie Gory, Moscow, Russia.

Corresponding author: F. Demory, CEREGE, Europôle de l'Arbois, BP80, 13545 Aix en Provence, France. (demory@cerege.fr)

0094-8276/13/10.1002/grl.50763

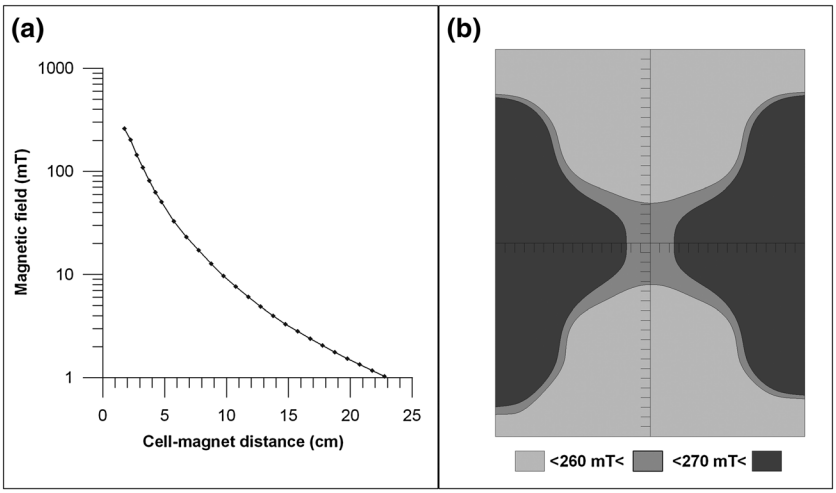

Figure 1. (a) Magnetic field generated at the center of the pair of permanent magnets in the IRM acquisition system designed to receive the pressure cell (see Figure S1) as a function of distance from center to magnet face. (b) Cross section of the magnetic field strength for the closest distance between magnets. The area with homogeneous field is 5 mm large for 8 mm high. The field in the center of the frame was measured using a Hall Effect Probe (GM08, Hirst Magnetic Instruments Limited).

pseudo-single domain (PSD) titanomagnetite (bba) composed of two equal phases with different substitution rate (0.8 and 0.6), PSD titanomagnetite (be-3a) with a substitution rate of 0.5, near single domain (SD) titanomagnetite (kil-2) with a substitution rate of 0.6, multidomain (MD) magnetite (est), and MD pyrrhotite (pyr-a). For MD hematite (BG-8603), we selected a sample of banded iron formation (Ouabego, M., Y. Quesnel, P. Rochette, F. Demory, E. M. Fozing, T. Njanko, J.-C. Hippolyte, and P. Affaton, Rock magnetic investigation of possible sources of the Bangui magnetic anomaly, submitted to *Physics of the Earth and Planetary Interiors*, 2013). Hematite was confirmed by a large Morin transition and typical hysteresis. Except pyr-a, which is a sized fraction from *Dekkers* [1988] embedded in epoxy, all other selected samples are natural rocks dominated by a well characterized magnetic mineralogy [*Bezaeva et al*., 2010, and references therein]. All samples (except BG-8603) were already subject to hydrostatic pressure (up to 1.2 GPa) demagnetization of IRM acquired at atmospheric pressure [*Bezaeva et al*., 2010]. The possible effects of this preliminary study are discussed in section 4. All samples are soft enough to be nearly saturated in 260 mT. The initial data of *Bezaeva et al*. [2010], the description of samples, and the results of the present study are compiled in table S1 presented in supporting information.

[6] To apply hydrostatic pressures, samples were inserted in a nonmagnetic pressure cell containing a liquid pressure transmitting medium (polyethilsiloxane liquid PES-1) providing effective hydrostatic conditions up to 1.8 GPa at room temperature [*Kirichenko et al*., 2005; *Sadykov et al*., 2008]. Samples have variable shape (some are roughly spherical and some are cylindrical; see masses in the table in supporting information) and occupy much less than 50% of chamber volume. The fact that the samples are fully surrounded by a liquid phase ensures that they are submitted at their borders to pure hydrostatic pressure. As the samples are polyphasic assemblage of solid phases with different and eventually anisotropic compressibilities, some deviatoric stresses may exist at microscopic scale. Therefore, the pure hydrostatic conditions refer to the pressure applied on the bulk sample, not necessarily to the microscopic scale. The pressure was applied following the protocol of *Bezaeva et al*. [2010] using a SPECAC press and a piston of 7 mm diameter. The pressure was cross-calibrated with another cell that was calibrated using a manganin sensor [*Sadykov et al*., 2008]. For 1 ton of applied force, the effective pressure in the cell is 0.23 GPa. The maximum loading in the present study is 6 tons, with a corresponding pressure of 1.4 GPa. Considering the unknown repeatability of the calibration versus loading condition and the precision of the press gauge, we estimate that uncertainty on pressure is about 5%. To impart IRM to the samples under pressure in the cell, we used an aluminum frame holding face to face two mobile rare earth magnets of 40 mm diameter (see Figure S1). The pressure cell, guided by the plastic rails, is placed at the center of the frame with the magnets initially placed at 24 cm from the center. In this configuration, the residual field in the center does not exceed 1 mT (Figure 1a). The distance between magnets is then reduced to 4 cm to produce a magnetic field of 260 mT at the center (Figure 1a). At closest position, the volume in which the magnetic field is homogeneous (i.e., between 260 and 270 mT) is 5 mm large and 8 mm high (Figure 1b). The magnets are then moved away back to their initial position and the pressure cell removed from the system. Field gradients in the sample zone decreases rapidly as a function of magnet distance. The hydrostatic chamber is 6.9 mm large and 20 mm high, and the samples, much smaller than the chamber (the biggest sample is 8 mm high for 5 mm large and its long axis is placed in vertical position), are centered. Therefore, all samples are affected by a homogeneous field within the cell.

[7] To demagnetize IRM_{260mT}, the pressure cell was again placed in the center of the aluminum frame but in the opposite direction to the IRM_{260mT} acquisition, and the distance between magnets was decreased step by step. IRM_{260mT} and its stepwise demagnetization were measured by placing the hydrostatic pressure cell in a superconducting rock magnetometer with a moment sensitivity of $\sim 10^{-11}$ Am^2 (SRM760R, 2G Enterprises). A Micromag vibrating sample magnetometer (VSM) with 1 T maximum field was used for hysteresis

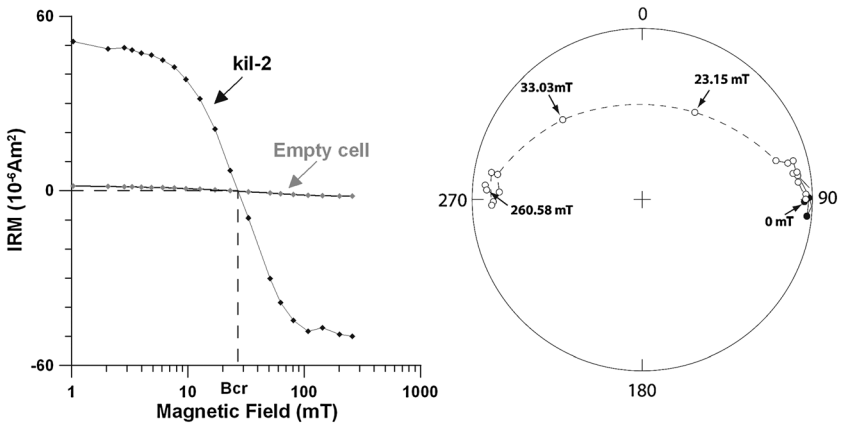

Figure 2. Results of backfield magnetization experiment for sample kil-2 at 0 GPa. (left) IRM produced with a field of 260 mT (IRM_{260mT}) versus backfield intensity showing B_{cr} determination. In grey is reported the backfield curve for the empty cell (subtracted from the sample measurements). (right) Stereographic projection showing the IRM direction as a function of backfield.

measurements after decompression (see Table S1). All experiments were carried out at Centre Européen de Recherche et d'Enseignement de Géosciences de l'Environnement.

3. Results

[8] Acquisition and stepwise demagnetization of the IRM_{260mT} were measured until the acquisition of the IRM_{260mT} in the opposite direction (Figure 2, left). For each sample measurement, the signal of the empty cell was subtracted. IRM curves for the empty cell are quite constant with pressure. IRM of the cell reaches a maximum of 1.88 10^{-6} Am^2 at 260 mT (Figure 2, left) that corresponds to 23.8 % of the signal of the weakest sample (MD magnetite est, Table S1). A first quality estimate was given by the absolute value of the IRM_{260mT} which has to be the same in both directions of acquisition. The quality of the demagnetization procedure was also estimated using stereographic projection of the resulting magnetic vectors showing the antipodality of the IRM_{260mT} acquired in the opposite field (Figure 2, right). B_{cr} could therefore be calculated from the demagnetization curve with good precision, as quantified by standard deviations calculated from repeated procedures.

[9] All samples except BG8603 were subjected to two compression-decompression experiments: the first one up to 1.2 GPa by *Bezaeva et al*. [2010] and the second one up to 1.4 GPa in the present study. The constant magnetic characteristics before the first compression and after the last decompression confirm that repeated hydrostatic pressure experiments up to 1.4 GPa do not affect irreversibly the magnetic properties, at odds with *Gilder and Le Goff* [2008] and *Gilder et al*. [2011] experiments for similar maximum pressures (Figure 3). Most of the changes observed on IRM intensity can be explained by the anisotropy of the samples which is quantified by a standard deviation resulting from IRM measurements and B_{cr} calculations performed at final stage in two or three perpendicular directions for all samples (see Table S1). The largest relative change reaches 11%. It concerns the IRM of the pyrrhotite sample (pyr-a) and may be attributed to its anisotropy reaching 20%. Few changes (none of them exceeding 10% of the IRM) can also be due to a slight loss of material related to friability of some samples (this is probably the case for hematite sample BG-8603). Concerning B_{cr}, only Be-3a presents a significant change with an increase of 25% mostly acquired during the compression-decompression experiment performed by *Bezaeva et al*. [2010]. As the sample is soft, the absolute change is only of 4.5 mT.

[10] The evolution of IRM_{260mT} with pressure shows complex behavior (Figure 4a). Mild variation (<10%) is shown by hematite (decrease) and PSD titanomagnetite (increase). SD titanomagnetite (Kil-2) shows first a decrease of the IRM_{260mT} of about 25% at 0.45 GPa, and then an increase at steps 0.9 and 1.4 GPa up to values equivalent to the magnetization before pressure experiment. This nonmonotonic behavior is unique among our data set. Interestingly, the same sample was the only one to show a distinct sigmoidal

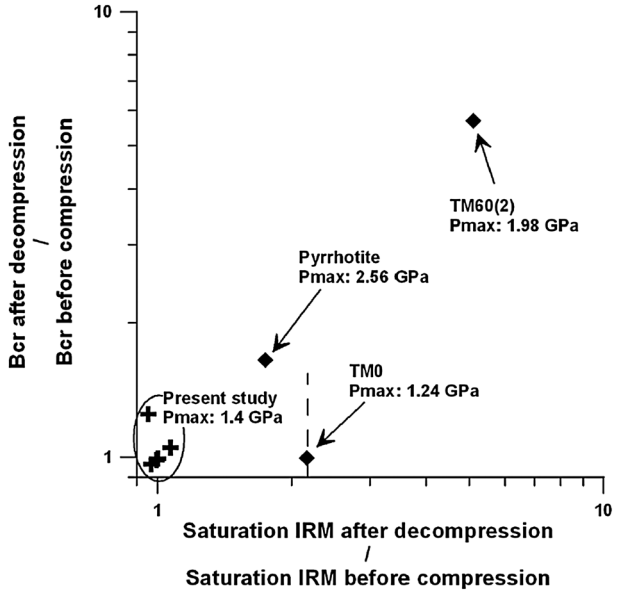

Figure 3. Relative change of B_{cr} versus relative change of IRM before compression and after decompression for five samples of the present study subject to two loading and unloading processes; the first by *Bezaeva et al*. [2010] up to 1.2 GPa and in the present study up to 1.4 GPa. The results for MD titanomagnetites [*Gilder and Le Goff*, 2008] and pyrrhotite [*Gilder et al*., 2011] subject to moderate loading are also plotted for comparison. Note that B_{cr} has not been determined for TM0.

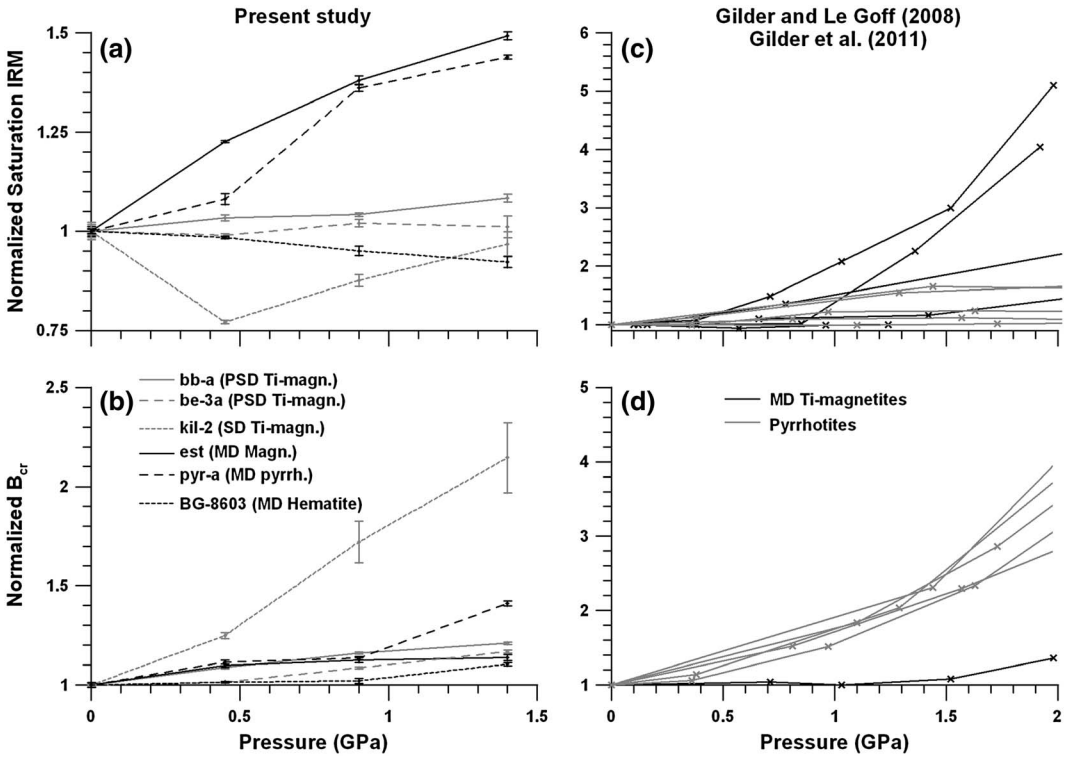

Figure 4. (a and b) Evolution of IRM at 260 mT (IRM_{260mT}) and B_{cr} with pressure for the six studied samples. Repeatability tests allowed adding error bars to the figures (+/− standard deviation). (c and d) To compare our results with the results obtained with solid confining media, data from *Gilder and Le Goff* [2008] conducted on MD titanomagnetites and from *Gilder et al*. [2011] conducted on pyrrhotites are plotted. The graphs focus on the range of pressure between 0 and 2 GPa in order to facilitate the comparison. Note that B_{cr} of only one MD titanomagnetite (TM 60(2)) was present in *Gilder and Le Goff* [2008].

shape of IRM demagnetization curve, with an inflection point near 0.4 GPa [*Bezaeva et al*., 2010]. This may sign the competition of two pressure sensitive processes. MD magnetite (est) and pyrrhotite samples display a large progressive increase of IRM_{260mT} up to 40–50% of the original value at 1.4 GPa.

[11] All samples show a regular increase of coercivity under pressure (Figure 4b), with the least effect shown by hematite followed by MD magnetite and PSD titanomagnetite samples, all with relative increases at 1.4 GPa below 20%. Larger effects are observed for pyrrhotite (40%) and SD titanomagnetite (110%).

4. Discussion

[12] The use of a hydrostatic pressure cell prevents irreversible deformation of the sample so that initial rock magnetic characteristics are preserved after decompression (Figure 3). This result is important because deformation may cause strong changes in rock magnetic characteristics [e.g., *Gattacceca et al*., 2007]. This nonhydrostaticity is discussed in a recent paper [*Gilder et al*., 2011] and likely explains the strong and nonreversible increase of the IRM and coercivity measured after decompression, as demonstrated in Figure 3.

[13] Under pressure, the magnetic signature of deformation as well as of deviatoric stress cannot be separated from the effect of the hydrostatic pressure itself, thus rendering the interpretation of previous experiments with solid confinement ambiguous. For MD magnetite and pyrrhotite, we qualitatively reproduced the increase of IRM and B_{cr} under pressure reported by *Gilder and Le Goff* [2008] and *Gilder et al*. [2011], but to a lesser extent. The discrepancy is, for example, obvious for the IRM of some titanomagnetite and the B_{cr} of pyrrhotite (Figures 4c and 4d). The increase in coercivity is attributed to changes in the crystalline anisotropy and therefore in the magnetostrictive anisotropy [*Kamimura et al*., 1992; *Gilder et al*., 2011]. The present study shows that part of this change is reversible and purely due to the effect of hydrostatic pressure. Another difference between the two sets of experiments for (titano-)magnetite is that *Gilder and Le Goff* [2008] used highly concentrated assemblages of magnetic crystals, while our experiments on rocks ensure a much lower potential effect of magnetic interactions, which are known to strongly affect coercivity and remanence for magnetite [*Sugiura*, 1979].

[14] Our PSD titanomagnetites (bb-a and be-3a) display constant IRM_{260mT} whatever the hydrostatic pressure applied. This result differs strongly from pressure experiments conducted by *Gilder and Le Goff* [2008], reporting an increase of the IRM by a factor up to three for MD titanomagnetite in equivalent pressure applications. This difference may be again partially attributed to deviatoric stress and strain. In addition, the present study deals with pseudo single domains whereas *Gilder and Le Goff* [2008] deal with multidomains so that changes of domain state during under pressure could play a role in the magnetization enhancement. Magnetic domain reorganization may explain the increase of B_{cr} of about 10% observed in the present study.

[15] The increase by a factor two of B_{cr} for SD titanomagnetite (kil-2) is coherent with the results of *Gilder et al*. [2004]. On the other hand, the present study shows first a decrease at low pressure and an IRM_{260mT} at 1.4 GPa equivalent to the IRM_{260mT} at 0 GPa whereas *Gilder et al*. [2004] report a strong increase of more than twice the original magnetization at 1.5 GPa. This strong increase may again be related to magnetic mineral deformation as the magnetization after decompression is 60% to 80% higher than magnetization before the experiments of *Gilder et al*. [2004].

[16] The slight decrease of IRM_{260mT} (Figure 4a) for the MD hematite sample (BG-8603), at odds with the behavior of MD magnetite and pyrrhotite, may be related to the Morin transition. Indeed, it has been observed that the temperature of the Morin transition increases with pressure of about 30°C per GPa [*Parise et al*., 2006]. The measurements performed at 1.4 GPa and at room temperature are close to the transition from antiferromagnetism to paramagnetism, that would explain the decrease of the IRM_{260mT}, pressure application being somehow equivalent to cooling near the Morin transition [*Özdemir et al*., 2008]. However, the relationship between pressure and Morin transition temperature needs to be better constrained (ongoing study with our pressure cell).

5. Conclusion

[17] The pressure experiments conducted using a liquid confining media pressure cell up to 1.4 GPa show that magnetic properties come back to their original values after decompression, contrary to previous studies conducted with solid confining media. Since this procedure avoids permanent deformation and deviatoric stress, the evolution of magnetic properties is therefore only induced by the effect of hydrostatic pressure and is thus a better analog of the in situ conditions at large depths. We confirm the general increase of remanent coercivity under pressure previously observed on magnetite, titanomagnetite, and pyrrhotite, but to a much lower extent than observed in nonhydrostatic pressure: this increase remains below 20% up to 1.4 GPa (except for MD pyrrhotite and SD titanomagnetite, with 30 and 110%, respectively). Saturation remanence increases by more than 5% only for MD magnetite and pyrrhotite (up to 50%), but again much less than in previous experiments. Still, these changes must be taken into account for estimating the deep in situ magnetizations. However, one needs also to predict the combined effect of pressure and temperature. These increases support again the need for taking into account geologically stable remanence in deep crustal magnetization modeling [*Shive*, 1989; *McEnroe et al*., 2004]. Hematite, studied for the first time at such pressures, as well as SD titanomagnetite, may show a decrease of saturation remanence under pressure. Our results are also the first obtained in that pressure range on rocks with diluted magnetic grains rather than on assemblages of strongly interacting crystals.

[18] **Acknowledgments.** We thank M. Fuller and S. Gilder for their reviews, which helped to improve the submitted manuscript.

[19] The Editor thanks an anonymous reviewer and Stuart Gilder for their assistance in evaluating this paper.

References

Arkani-Hamed, J., and D. Strangway (1987), An interpretation of magnetic signatures of subduction zones detected by MAGSAT, *Tectonophysics*, *133*, 45–55, doi:10.1016/0040-1951(87)90279-4.

Bezaeva, N. S., J. Gattacceca, P. Rochette, R. A. Sadykov, and V. I. Trukhin (2010), Demagnetization of terrestrial and extraterrestrial rocks under hydrostatic pressure up to 1.2 GPa, *Phys. Earth Planet. In.*, *179*, 7–20, doi:10.1016/j.pepi.2010.01.004.

Borradaile, G. J. (1997), Deformation and paleomagnetism, *Surv. Geophys.*, *18*, 405–435.

Dekkers, M. J. (1988), Magnetic properties of natural pyrrhotite, part 1: Behaviour of initial susceptibility and saturation-magnetization related rock magnetic parameters in a grain-size dependent framework, *Phys. Earth Planet. In.*, *52*, 376–393, doi:10.1016/0031-9201(88)90129-X.

Dunlop, D. J., and J. Arkani-Hamed (2005), Magnetic minerals in the Martian crust, *J. Geophys. Res.*, *110*, E12S04, doi:10.1029/2005JE002404.

Frost, B. R., and P. N. Shive (1986), Magnetic mineralogy of the lower continental crust, *J. Geophys. Res.*, *91*, 6513–6522, doi:10.1029/JB091iB06p06513.

Gattacceca, J., A. Lamali, P. Rochette, M. Boustie, and L. Berthe (2007), The effects of explosive-driven shocks on the natural remanent magnetization and the magnetic properties of rocks, *Phys. Earth Planet. In.*, *162*, 85–98, doi:10.1016/j.pepi.2007.1003.1006.

Gilder, S., and M. Le Goff (2008), Systematic pressure enhancement of titanomagnetite magnetization, *Geophys. Res. Lett.*, *35*, L10302, doi:10.1029/2008GL033325.

Gilder, S. A., M. Le Goff, J. Peyronneau, and J. C. Chervin (2002), Novel high pressure magnetic measurements with application to magnetite, *Geophys. Res. Lett.*, *29*(10), 1392, doi:10.1029/2001GL014227.

Gilder, S. A., M. Le Goff, J. Peyronneau, and J. C. Chervin (2004), Magnetic properties of single and multi-domain magnetite under pressures from 0 to 6 GPa, *Geophys. Res. Lett.*, *31*, L10612, doi:10.1029/2004GL019844.

Gilder, S. A., R. Egli, R. Hochleitner, S. C. Roud, M. W. R. Volk, M. Le Goff, and M. de Wit (2011), Anatomy of a pressure-induced, ferrimagnetic to paramagnetic transition in pyrrhotite: Implications for the formation pressure of diamonds, *J. Geophys. Res.*, *116*, B10101, doi:10.1029/2011JB008292.

Kamimura, T., M. Sato, and H. Takahashi (1992), Pressure-induced phase transition in Fe-Se and Fe-S systems with a NiAs-type structure, *J. Magn. Magn. Mater.*, *104–107*, 255–256, doi:10.1016/0304-8853(92)90787-O.

Kirichenko, A. S., A. V. Kornilov, and V. M. Pudalov (2005), Properties of polyethylsiloxane as a pressure-transmitting medium, *Instrum. Exp. Tech.*, *48*(6), 813–816, doi:10.1007/s10786-005-0144-5.

Martin, R. J., and J. S. Noel (1988), The influence of stress path on thermoremanent magnetization, *Geophys. Res. Lett.*, *15*(5), 507–510, doi:10.1029/GL015i005p00507.

McEnroe, S. A., F. Langenhorst, P. Robinson, G. Bromiley, and C. Shaw (2004), What's magnetic in the lower crust?, *Earth Planet. Sci. Lett.*, *226*, 175–192, doi:10.1016/j.epsl.2004.07.020.

Melosh, H. J. (1989), *Impact Cratering. A Geologic Process*, pp. 245, Oxford Monographs on Geology and Geophysics Series no 11, Oxford, United Kingdom.

Nagata, T. (1966), Main characteristics of piezo-magnetization and their qualitative interpretation, *J. Geomag. Geoelec.*, *18*, 81–97.

Özdemir, Ö., D. J. Dunlop, and T. S. Berquó (2008), Morin transition in hematite: Size dependence and thermal hysteresis, *Geochem. Geophys. Geosyst.*, *9*, Q10Z01, doi:10.1029/2008GC002110.

Parise, J. B., D. R. Locke, C. A. Tulk, I. Swainson, and L. Cranswick (2006), The effect of pressure on the Morin transition in hematite (alpha-Fe2O3), *Physica B- Condens. Matter*, *385*, 391–393, doi:10.1016/j.physb.2006.05.081.

Pozzi, J. P. (1975), Magnetic properties of oceanic basalts effects of pressure and consequences for the interpretation of anomalies, *Earth Planet. Sci. Lett.*, *26*, 337–344, doi:10.1016/0012-821X(75)90009-6.

Revol, J., R. Day, and M. Fuller (1977), Effect of uniaxial compressive stress upon remanent magnetization: Stress cycling and domain state dependence, *J. Geomag. Geoelec.*, *30*, 593–605.

Sadykov, R. A., N. S. Bezaeva, A. I. Kharkovskiy, P. Rochette, J. Gattacceca, and V. I. Trukhin (2008), Nonmagnetic high pressure cell for magnetic remanence measurements up to 1.5 GPa in a superconducting quantum interference device magnetometer, *Rev. Sci. Instrum.*, *79*, 115102, doi:10.1063/1.2999578.

Shive, P. N. (1989), Can remanent magnetisation in the deep crust contribute to long wavelength magnetic anomalies?, *Geophys. Res. Lett.*, *16*(1), 89–92, doi:10.1029/GL016i001p00089.

Sugiura, N. (1979), ARM, TRM and magnetic interactions: Concentration dependence, *Earth Planet. Sci. Lett.*, *42*, 451–455, doi:10.1016/0012-821X(79)90054-2.

Voorhies, C. V., T. J. Sabaka, and M. Purucker (2002), On magnetic spectra of Earth and Mars, *J. Geophys. Res.*, *107*(E6), 5034, doi:10.1029/2001JE001534

Wu, T.-C., and W. A. Bassett (1993), Deviatoric stress in a diamond anvil cell using synchrotron radiation with two diffraction geometries, *Pure Appl. Geophys.*, *141*(2-4), 509–519, doi:10.1007/BF00998343.